RAPID POINT-OF-CARE LFA DIAGNOSTICS FOR ORAL HEALTH USING OPTICAL EXCITATION/DETECTION METHODS

Daewoo Han[1], Der Vang[2], Adewale Adehinmoye[2], Lyndsay Kissell[2], Pietro Strobbia[2] and Andrew J. Steckl[1]*
[1] Department of Electrical and Computer Engineering, University of Cincinnati, Cincinnati, OH 45221
[2] Department of Chemistry, University of Cincinnati, Cincinnati, OH 45219 USA

ABSTRACT

We report a point-of-care (POC) lateral flow immunoassay (LFA) with enhanced sensitivity achieved by adapting surface-enhanced Raman scattering (SERS) technique for detecting *P. gingivalis*, a key oral health biomarker. Our SERS–LFA achieves a < 10 ng/mL limit of detection (LOD), ~ 10-fold higher than conventional LFAs. Portable Raman system designed for LFAs provided comparable results with benchtop equipment. This will bring SERS–LFA closer to POC use, facilitating oral health monitoring capabilities on sites. Herein, we discuss the material optimization and feasibility of thermal imaging on nanoparticles of the test line using IR camera enables more economical option for POC use.

KEYWORDS

Point-of-care, LFA, SERS, IR imaging, saliva, endotoxin, bacteria, oral health.

INTRODUCTION

Efficient and economical POC approach using various biofluids can offer early detection of medical conditions, enhancing treatment efficacy and reducing medical costs to patients.[1] As a POC platform, LFA demonstrated its versatility during the COVID pandemic, due to the rapid analysis, affordability, and user-friendly interface. Furthermore, the widespread adoption of LFA-based COVID home test kit leads to global familiarity with the use of LFAs. However, because current LFA tests could not fully detect pre-symptomatic infections, a new demand is rising to provide more accurate results with enhanced sensitivity.[2, 3]

Lipopolysaccharides (LPS), consisting of lipid A and polysaccharide components, are important macromolecules found in the outer layer of Gram-negative bacteria. Upon bacterial death or metabolic stress, a substantial number of LPS molecules are released. [4, 5] Once released, the toxic Lipid A component of LPS is exposed to the host's immune system. This exposure can trigger strong immune responses to the host, such as various inflammations, life-threatening sepsis, etc.[6]

Porphyromonas gingivalis (*P. gingivalis*), one of more than 700 bacterial species found in the oral cavity, is a major Gram-negative pathogenic bacterium that is closely related to the oral disease such as gingivitis and periodontitis. LPS from *P. gingivalis* (PG LPS) induces significant host responses in gingival tissue. It damages soft tissue and supporting bones for teeth, leading to tooth loss.[7] Furthermore, recent research presented the close relationship between *P. gingivalis* and the important systemic diseases such as cardiovascular[8], rheumatoid arthritis[9], and Alzheimer's disease[10].

We have previously developed[11] colorimetric LFA detection of PG LPS from human saliva to monitor the oral health status. The colorimetric detection limits (LODs) from the LFA were ~ 22 and 46.5 ng/mL for water-based and saliva samples, respectively. However, the endotoxin level of healthy individuals and periodontitis patients are ~10 and 30 ng/mL, respectively[12], indicating the need for more sensitive LFA detection. Recently, we adapted the developed LFA to be tested via surface-enhanced Raman scattering (SERS), to exploit the excellent sensitivity and multiplex analysis capability of this spectroscopy. Previous reports have shown that SERS-based LFA can be used to achieve higher sensitivities.[13] For example, Song et al. have optimized gold nanoparticles (AuNP), reaction time and buffer components to achieve a 78 times higher sensitivity than that of colorimetric results.[14] We further expanded this approach by investigating the role of different plasmonic nanomaterials (i.e., metallic nanostars) in the sensitivity improvement.[15]

Thermal imaging has also been used as a method to enhance sensitivity in LFA. These process involve the heating of the LFA strip with a laser beam and detection with a thermal camera.[16, 17] Because metallic NP have very high photothermal efficiency, they show significant heating even with short irradiation times. This method is an interesting alternative to SERS-LFA, as thermal imagers are more affordable compared to Raman detectors.

Interestingly, both these phenomena (SERS and NP photothermal conversion) are associated with the plasmonic properties of NP. Specifically, once a NP is illuminated with the light resonant with the specific localized surface plasmon (LSP), the LSP from the particle can relax by either releasing scattered light or heat, which are associated with SERS and photothermal heating, respectively. In our recent work, we optimized nanomaterials to maximize the SERS output for the LFA. Herein, we will study

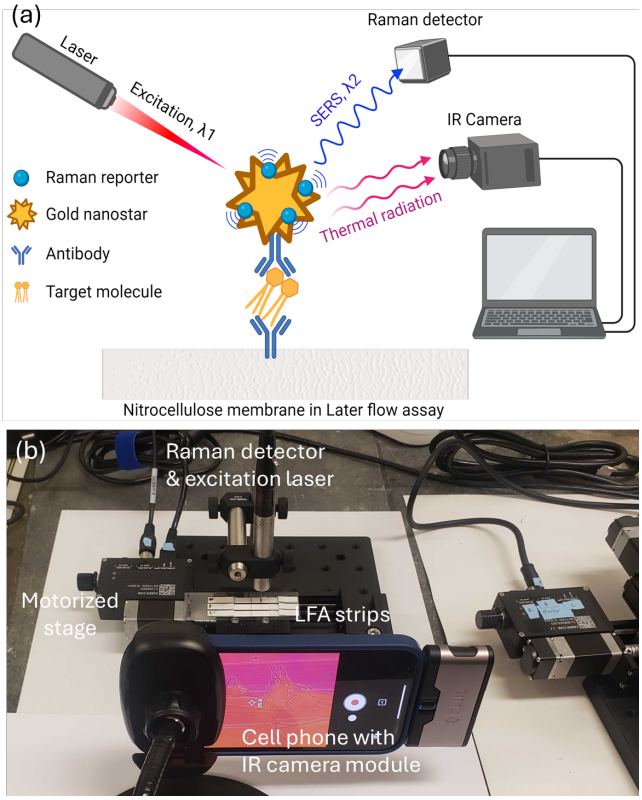

Figure 1: Measurements of SERS and thermal imaging detection on LFA test strips: (a) schematic of working mechanisms, (b) experimental configuration.

978-1-1940470-05-4/HH2024/$25©2024TRF
DOI 10.31438/TRF.HH2024.86

simultaneously SERS and thermal heating from different materials on LFA, to understand the optimization of each process.

Figure 1a shows the schematic of SERS and thermal detection mechanism on LFA strip. In the presence of target LPS in sample solution, antibodies on nanoparticles conjugated with a reporter molecule bind to the LPS first, and then bind to another antibody immobilized on the nitrocellulose membrane of LFA strip. When the conjugate is irradiated by the excitation laser, the reporter molecule absorbed on the surface of metal nanoparticles generates strong Raman scattering via SERS. Because of the strong electromagnetic field on metal nanoparticles, it generates the localized heat which can be detected by simple IR camera. Experimental setup of both SERS and thermal imaging is shown in Figure 1b. LFA strip is placed on the Labview-controlled motorized stage to scan the targeted LFA strip area. Laser and Raman detector is aligned vertically on top of the LFA strip. During the SERS measurement, thermal imaging is simultaneously taken using the cell phone connected with IR camera module.

Conventional LFA test results rely on the visual judgement of the color intensity of the test line formed by accumulated AuNPs under the immuno-reaction between target analytes and antibodies. Figure 2a shows the basic concept of our sandwich immunoassay on LFA. Sensitive sandwich immunoassay approach was adapted to LFA because LPS forms a large biomolecule providing multiple binding sites. Monoclonal antibody was conjugated to gold nanoparticles by physical absorption, and the polyclonal antibody is immobilized on nitrocellulose membrane of LFA device using BioDot printer. Once targeted LPS present, this conjugated AuNP binds to the LPS. After dispensing on sample pad, it flows through the nitrocellulose membrane and captured by second antibody which can bind to the different binding site of LPS. Eventually forming the colorimetric red line on LFA. Control line is detecting antibody on AuNP so that it confirms the validity of the test.

To generate the SERS signal, Raman reporter molecules, 1,1′,3,3,3′,3′-hexamethylindotricarbocyanine iodide (HITC), are

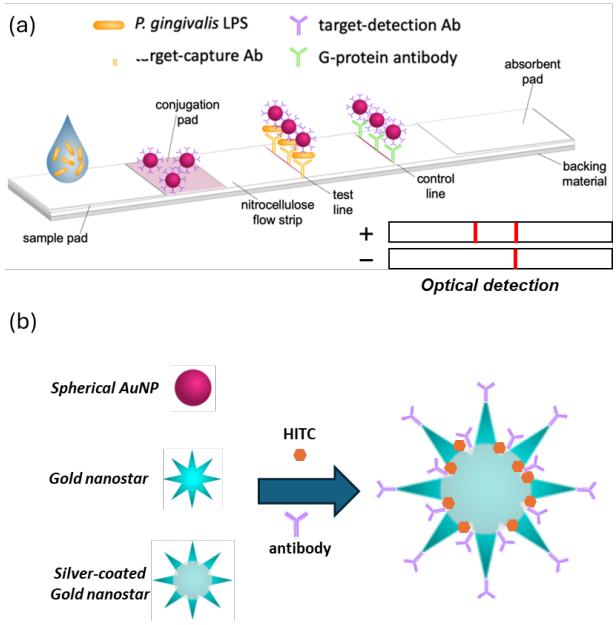

Figure 2: Schematic of SERS LFA for detecting P. gingivalis LPS: (a) colorimetric LFA configuration, (b) different nanomaterials replacing Au spheres and their representative SERS readout (T: test line, C: control line) from LFA test. Adapted from [15] with permission from Royal Society of Chemistry.

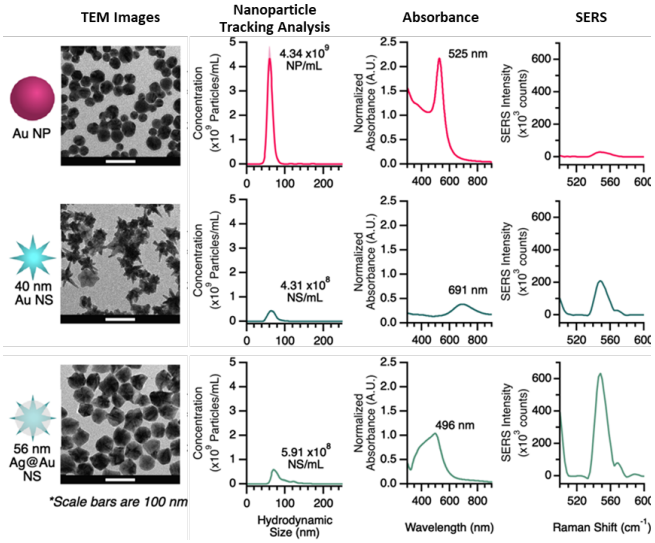

Figure 3: Characteristics of three different nanoparticles: (a) TEM images, (b) nanoparticle tracking analysis for particle density measurement, (c) UV-vis absorption spectrum, (d) SERS spectrum. Adapted from [15] with permission from Royal Society of Chemistry.

incorporated on the surface of metal nanoparticles (Figure 2b). For further enhanced sensitivity, gold nanostar (AuNS) was utilized instead of spherical AuNP. In our SERS-LFA, we have also utilized the silver (Ag)-coated AuNS presenting stronger Raman signal than that of pure AuNS. The star-shaped nanostructure is a very efficient plasmonic material, generating stronger SERS response than spherical nanomaterials. We have prepared various nanostars in different sizes and compositions (Figure 2b).

RESULTS

Nanoparticles analysis

The TEM observation (Figure 3a) clearly shows that AuNPs are spherical shape with average diameter of 37.3 nm, while AuNS with the tip-to-tip diameter of 40 nm display the highly branched nanostructure. The silver coated gold nanostar (Ag@AuNS) with a diameter of 56 nm appears somewhat round although the contrast in TEM image shows the branched AuNS structure is intact beneath the silver shell.

As shown in Figure 3b, nanoparticle tracking analysis (NTA) shows that the concentration of as-synthesized 39 nm Ag@Au NS is about 30-45% of commercially available spherical AuNP concentration. Similarly, as-synthesized 56 nm Ag@Au NS are only about 10-13% of the commercial AuNPs concentration. Although NTA measurements are relatively fast, it is not practical for measuring every sample. However, in conjunction with UV-vis absorption spectrum shown in Figure 3c, we can quickly evaluate the concentration of each type of nanomaterial using the absorption peak intensity, and adjust concentrations as needed for comparing nanomaterials.

SERS performance (Figure 3d) was initially conducted by measuring the Raman signal of HITC reporter-functionalized particles on the cellulose pad used for LFA. As expected, the spherical AuNPs presented the weakest SERS intensity. On the other hand, the 56 nm Ag@AuNS presented the strongest SERS signal intensity, which are 3.1 and 21.4 times higher than that of 40 nm AuNS, and spherical AuNP, respectively.

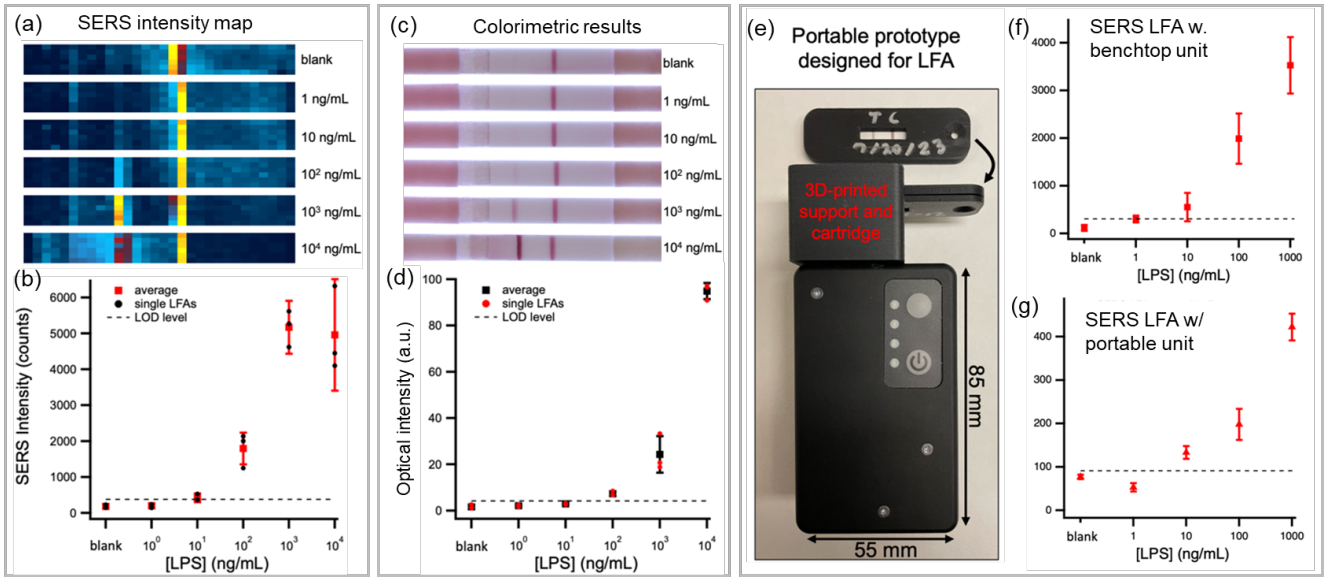

Figure 4: Characteristics of various nanoparticles: (a) TEM images, (b) nanoparticle tracking analysis for particle density measurement, (c) UV-vis absorption spectrum, (d) SERS spectrum. Modified from [15] with permission from Royal Society of Chemistry.

SERS detection on LFA

To evaluate LFA performances, different LPS concentrations were tested both on SERS-LFA and optical-LFA as shown in Figure 4. The Ag@AuNS and spherical AuNP were selected for SERS and colorimetric measurements, respectively. In SERS, the laser was scanning 6 times along the 30 mm LFA long-axis with 1 mm steps and the average value was calculated. The Raman colormap intensity at 549 cm^{-1} (Figure 4a) and the test line intensity as a function of LPS concentration (Figure 4b) were obtained.

Similarly, for colorimetric evaluation, photo of tested LFA with different LPS concentrations was taken (Figure 4c) and the analyzed optical intensity using ImageJ is plotted in Figure 4d. As shown in Figure 4b,d, While the colorimetric LFA detection presented the LOD level in the 20-100 ng/mL range, the SERS-LFA detection results show LOD level < 10 ng/mL. Clearly, SERS detection provides ~ 10-fold enhancement of the LFA sensitivity.

Enhanced sensitivity using SERS detection brings the LOD level to the clinically relevant range for LPS detection. However, a consideration in the translation to POC use of Raman systems is their complexity, size, and cost, which typically contains microscopes, benchtop laser and spectrometer equipment. To address this issue, hand-held portable Raman system has been developed for the use in POC applications. We have conducted testing using a portable SERS prototype, developed by Wasatch Photonics as shown in Figure 4e. This compact system with dimensions of 85 (L) × 55 (W) × 30 (T) mm can be operated on battery power. To enhance the Raman signal detection from the test line of LFA, the line-shaped laser excitation was utilized. The prototype includes a 3D-printed cartridge for convenient LFA strip reading and it seamlessly fits into the support unit, aligning the LFA test and control lines precisely within the laser's line focus points.

To evaluate the feasibility of the developed SERS–LFA technology in the portable SERS unit, we have compared the outcomes obtained from a benchtop and portable Raman systems, using a same set of LFA test strips with different concentrations of PG LPS. Results from the benchtop system (Figure 4f) and the portable device unit (Figure 4g) show very similar performance with the LOD level < 10 ng/mL. Interestingly, SERS measurements using

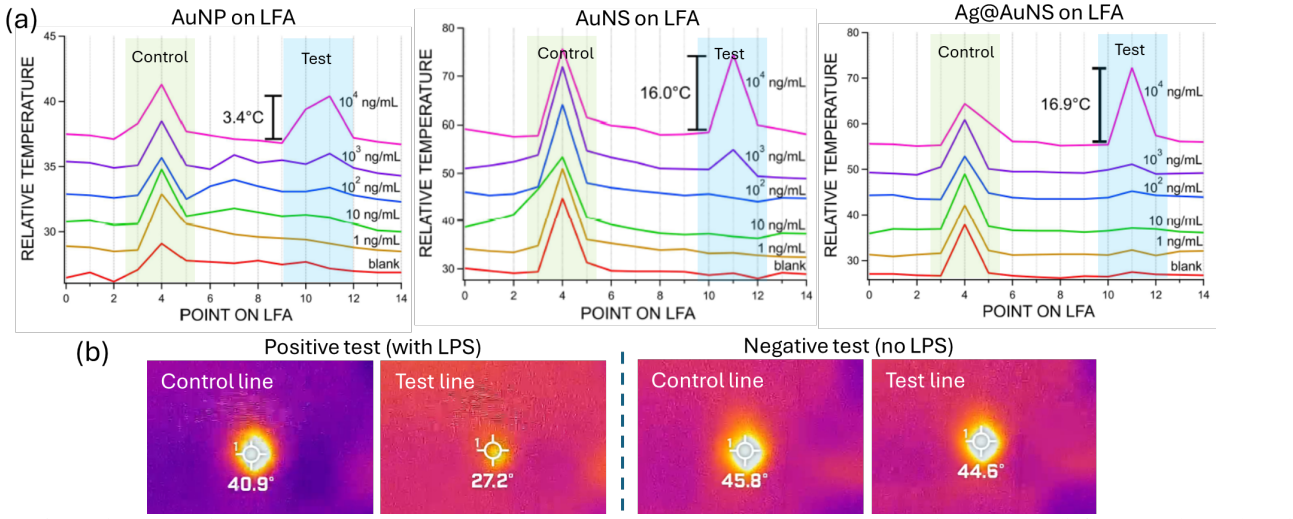

Figure 5: Thermal imaging detection on LFA test strips: (a) temperature changes on the LFA strip tested with AuNP (left), AuNS (center) and Ag@AuNS (right). (b) Thermal images taken by IR camera for negative and positive test results on LFA.

a portable device presented smaller variance compared to that on the benchtop system. This is possibly due to the measurement methodology. While the benchtop system has a manual operation for the laser alignment, all components in the portable device are pre-aligned and measurement done at a single laser scan, which is beneficial to improve the consistency.

Thermal imaging on LFA

The plasmonic photothermal properties of the nanostars can also be utilized as a relatively simple sensing methodology using an affordable IR camera to monitor the temperature change. Results shown in Figure 5a indicate that AuNS and Ag@AuNS induce a higher temperature increase of 16.0 and 16.9 °C, respectively, than the increase of 3.4 °C from AuNP. Thermal images are shown in Figure 5b. For the negative case with no LPS, only control line generates the local heating to 40.9 °C. On the other hand, for the positive test, localized heating was observed for both control and test lines. Temperature values were taken after 10 sec of laser exposure. Because of the close relationship between SERS and thermal effects, the stronger SERS signal observed in nanostars compared to nanospheres leads to the higher temperature increase. However, unlike in the SERS data of Figure 3, where silver coating produced a large increase in SERS signal, for the thermal imaging the uncoated nanostars produced comparable thermal effects. This observation is related to mechanisms of the photons interacting with the nanostars that can produce either heating or scattering. Silver coating increases the scattering efficiency but does not improve the photothermal efficiency.

CONCLUSION

This work discusses the optimization of materials for LFA with different optical detection methodologies. Our work demonstrates how the optimization of NPs needs to take into account the detection methodology to impact LFA sensitivities. By incorporating optimized nanomaterials and portable measurements, this technology can greatly improve the quality of clinical POC diagnostics for detecting PG LPS and potentially other important biomarkers.

ACKNOWLEDGEMENTS

The authors gratefully appreciate Dr. Sancai Xie from Procter and Gamble Co. for providing antibodies and many useful discussions on LPS detection. Also, the authors thank Wasatch Photonics for providing the prototype portable Raman system.

REFERENCES

[1] A. J. Steckl and P. Ray, "Stress Biomarkers in Biological Fluids and Their Point-of-Use Detection," *ACS Sensors,* 3, 2025-2044, (2018).

[2] J. Budd *et al.*, "Lateral flow test engineering and lessons learned from COVID-19," *Nat. Rev. Bioeng.,* 1, 13-31, (2023).

[3] Y. Liu, L. Zhan, Z. Qin, J. Sackrison, and J. C. Bischof, "Ultrasensitive and Highly Specific Lateral Flow Assays for Point-of-Care Diagnosis," *ACS Nano,* 15, 3593-3611, (2021).

[4] C. R. Raetz and C. Whitfield, "Lipopolysaccharide endotoxins," (in eng), *Annu Rev Biochem,* 71, 635-700, (2002).

[5] S. H. Rhee, "Lipopolysaccharide: Basic Biochemistry, Intracellular Signaling, and Physiological Impacts in the Gut," *Intest. Res.,* 12, 90-95, (2014).

[6] B. S. Park and J.-O. Lee, "Recognition of lipopolysaccharide pattern by TLR4 complexes," *Exp. Mol. Med.,* 45, e66-e66, (2013).

[7] J. Mysak *et al.*, "Porphyromonas gingivalis: Major Periodontopathic Pathogen Overview," *J. Immunol. Res.,* 2014, 476068, (2014).

[8] J. L. C. Mougeot, C. B. Stevens, B. J. Paster, M. T. Brennan, P. B. Lockhart, and F. K. B. Mougeot, "Porphyromonas gingivalis is the most abundant species detected in coronary and femoral arteries," *J. Oral Microbiol.,* 9, 1281562, (2017).

[9] B. Rodríguez-Lozano *et al.*, "Association between severity of periodontitis and clinical activity in rheumatoid arthritis patients: a case–control study," *Arthritis Res. Ther.,* 21, 27, (2019).

[10] S. S. Dominy *et al.*, "Porphyromonas gingivalis in Alzheimer's disease brains: Evidence for disease causation and treatment with small-molecule inhibitors," *Sci. Adv.,* 5, eaau3333, (2019).

[11] D. Han, S. Xie, and A. J. Steckl, "Salivary endotoxin detection using combined mono/polyclonal antibody-based sandwich-type lateral flow immunoassay device," *Sensors & Diagnostics,* 2, 1460-1468, (2023).

[12] S. Zaric *et al.*, "Evaluating clinical utility of subgingival and salivary endotoxin activity levels as periodontal biomarkers," (in eng), *Front Oral Health,* 3, 1029806, (2022).

[13] K. Kim *et al.*, "Recent advances in sensitive surface-enhanced Raman scattering-based lateral flow assay platforms for point-of-care diagnostics of infectious diseases," *Sensors and Actuators B: Chemical,* 329, 129214, (2021).

[14] E. Song, I. Kim, C. Jeon, and S. Pyun, "Development and optimization of surface-enhancement Raman scattering-based lateral flow immunoassays for the ultrasensitive detection of cardiac troponin I," *Microchemical Journal,* 193, 108962, (2023).

[15] L. N. Kissell, D. Han, D. Vang, A. W. R. Cikanek, A. J. Steckl, and P. Strobbia, "Improved point-of-care detection of P. gingivalis using optimized surface-enhanced Raman scattering in lateral flow assays," *Sensors & Diagnostics,* 10.1039/D4SD00056K (2024).

[16] Y. Liu, L. Zhan, J. Kangas, Y. Wang, and J. Bischof, "Fast and ultrafast thermal contrast amplification of gold nanoparticle-based immunoassays," *Sci. Rep.,* 12, 12729, (2022).

[17] Y. Wang *et al.*, "Thermal Contrast Amplification Reader Yielding 8-Fold Analytical Improvement for Disease Detection with Lateral Flow Assays," *Anal. Chem.,* 88, 11774-11782, (2016).

CONTACT

*A. J. Steckl - a.steckl@uc.edu

Celebrating 40 Years of Hilton Head!

GENERAL CHAIR:
JENNA F. CHAN
DEVCOM ARMY RESEARCH LABORATORY, USA

PROGRAM CHAIR:
SWAMINATHAN RAJARAMAN
UNIVERSITY OF CENTRAL FLORIDA, USA

TRF CATALOG NUMBER 24TRF-0001
ISBN NUMBER: 978-1-1940470-05-4
ISSN: 1539-204X (ELECTRONIC)
DOI 10.31438/TRF.HH2024.0

HH2024.ORG

SPONSORED BY

TRF TRANSDUCER RESEARCH FOUNDATION
connecting big ideas and small tech

CORPORATE STEWARDSHIP SPONSORS
NXP TDK InvenSense